Pinning Control in Networks of Nonidentical Systems With Many-Body Interactions

Roberto Rizzello and Pietro De Lellis

***Abstract*—We study the problem of controlling an ensemble of nonidentical dynamical units to a desired trajectory set by the pinner in the presence of multi-body interactions across the units. We provide sufficient conditions for local bounded convergence, and estimate the convergence bound as a function of the parameter mismatch between the units, and of the directed hypergraph describing their interacting topology. Numerical examples demonstrate the robustness of the approach.**

***Index Terms*—Pinning control, higher-order interactions, directed hypergraphs, opinion dynamics, networks.**

I. Introduction

In the last decades, the control of network systems has attracted a wide and interdisciplinary research effort [1], [2]. Namely, the control mechanisms that induce the emergence of collective behaviours, such as consensus and synchronization [3], [4], have been investigated. For instance, swarms of drones with limited computational abilities need distributed strategies to coordinate their motion [5], and leader-follower schemes are employed to drive fleets of unmanned vehicles [6]. Control applications are also in socioeconomics, when studying herding in opinion dynamics [7], or the design of optimal policies to regulate migration dynamics [8].

Graph theory has been effectively combined with dynamical systems to explain how pairwise interactions between the units of a network system enable the propagation of control signals [1]. An effective strategy is pinning control, where a pinner node, which can be viewed as the network leader, steers the trajectory of the network through a feedback action exerted on a small fraction of the follower nodes [9]. The dynamics of the i-th unit in a pinning controlled network is

$$\begin{aligned} \dot{x}_i &= f(x_i) + \sum_{j\in\mathcal{N}_i} \sigma_{ij} g\big(y_j - y_i\big) + q_i k_i g(y_{N+1} - y_i) \\ y_i &= \gamma(x_i), \qquad\qquad i = 1,\ldots,N \end{aligned} \tag{1a}$$

$$\dot{x}_{N+1} = f(x_{N+1}), \qquad\qquad y_{N+1} = \gamma(x_{N+1}) \tag{1b}$$

where $f : \mathbb{R}^n \to \mathbb{R}^n$ describes the individual dynamics of each node, $g : \mathbb{R}^m \to \mathbb{R}^n$ is the inner coupling function such that $g(0) = 0$, $\mathcal{N}_i$ is the set of in-neighbors of node i, $\sigma_{ij} > 0$ is the coupling strength associated to the pair (i, j), $\gamma : \mathbb{R}^n \to \mathbb{R}^m$ is the output function, and $y_i \in \mathbb{R}^m$ is the output of node i; the pinner, node $N + 1$, sets the reference trajectory and injects a control action that is proportional to the output error, with control gain k_i; the binary variable q_i is 1 if node i is *pinned* (*i.e.*, receives the input), whereas it is 0 otherwise. In the literature, conditions for successfully pinning control of network systems coupled over digraphs have been obtained when the individual dynamics are one-sided Lipschitz, the coupling and control gains are large enough, and a control signal is injected into at least a node for each root strongly connected component of the graph [10].

However, in control problems one needs to account for the unavoidable parametric mismatches that arise in applications, where the units can only be nominally identical, and the function f in (1) has different parameters for each node. In this context, proportional control actions as in (1) can only enforce bounded synchronization onto the desired, nominal trajectory [11], [12], [13]. In addition, limitation on sensing and actuation may render the coupling protocol in (1) unfeasible, thus requiring the use of hypergraph models [14], [15]. For instance, in microbial consortia feedback control is exerted based on fluorescence [16]. However, only an aggregated measurement of the fluorescence of a group of cells is available. Therefore, the control signal will be represented as an hyperedge from a virtual node (the tail of the hyperedge) setting the reference fluorescence, to the nodes of which we measure the aggregated fluorescence (the heads of the hyperedge). Additionally, hypergraphs are also needed to capture interaction protocols that involve more than two nodes. This is the case, for instance, of the study of battery charges, whereby the equalizers are viewed as hyperedges connecting more than two nodes, that is, more than two battery cells [17]. In such cases, the standard feedback protocol (1) cannot be implemented, and feedback mechanisms based on aggregated measurements of groups of nodes can be interpreted as many-body interactions and modeled through directed hypergraphs [18], [19], [20], see Fig. 1.

Albeit strongly motivated by applications, existing results on networks of heterogeneous systems with many-body interactions are only limited to special dynamics, such as for instance the Kuramoto model, where it was shown that richer transitions to synchronization emerge in the presence of higher-order interactions, see, e.g., [21]. In this letter,

Manuscript received 5 March 2024; revised 30 April 2024; accepted 27 May 2024. Date of publication 30 May 2024; date of current version 24 June 2024. This work was supported by the 2022K8EZBW "Higher-Order Interactions in Social Dynamics With Application to Monetary Networks" Project—funded by European Union—Next Generation EU within the PRIN 2022 Program (D.D. 104 - 02/02/2022 Ministero dell'Universitá e della Ricerca). Recommended by Senior Editor S. Tarbouriech. *(Corresponding author: Pietro De Lellis.)*

Roberto Rizzello is with the Department of Electrical Engineering and Information Technology, University of Naples Federico II, 80125 Naples, Italy, and also with SATIS Centre, 00198 Rome, Italy.

Pietro De Lellis is with the Department of Electrical Engineering and Information Technology, University of Naples Federico II, 80125 Naples, Italy (e-mail: pietro.delellis@unina.it).

Digital Object Identifier 10.1109/LCSYS.2024.3406916

© 2024 The Authors. This work is licensed under a Creative Commons Attribution 4.0 License.
For more information, see https://creativecommons.org/licenses/by/4.0/

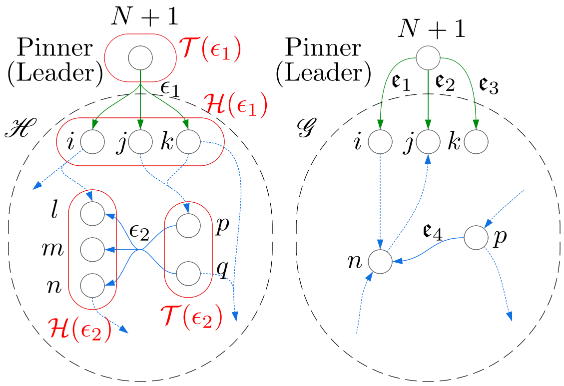

Fig. 1. Pinning control over a directed hypergraph $\mathscr{H}$ (left) and a digraph $\mathscr{G}$ (right). Each hyperedge is composed by a set of tails and a set of heads. For instance, $\mathcal{T}(\epsilon_2) = \{p, q\}$ and $\mathcal{H}(\epsilon_2) = \{l, m, n\}$. The pinner (leader) is the sole tail of the hyperedge ϵ_1 and only measures an aggregated output $y_{ijk} = (\tilde{\beta}_\epsilon)_i y_i + (\tilde{\beta}_\epsilon)_j y_j + (\tilde{\beta}_\epsilon)_k y_k$ of the head nodes i, j, and k, and will inject a signal $g(y_{N+1} - y_{ijk})$ function of the state of all 4 nodes of the hyperedge ϵ_1. g will be in general nonlinear, and therefore not decomposable as sum of pairwise interactions. Differently, a standard edge has only one tail and one head, and the pinner in the right panel will be able to individually measure the state of i, j, and k. For instance, it will inject the signal $g(y_{N+1} - y_i)$ at node i through the standard edge $\mathfrak{e}_1$.

we are the first to provide, for general nonlinear dynamics, convergence results for pinning control of networks of non-identical systems in the presence of higher order interactions. Specifically, we provide i) analytical conditions on the hypergraphs that describes the many-body interactions, on the set of pinned nodes, and on the coupling and control gains to attain local bounded pinning controllability, ii) a convergence bound that is rigorously valid for infinitesimal perturbations with respect to the reference trajectory and nominal parameters, and iii) numerical evidence that this bound is robust to the presence of large perturbations.

Notation: Given $n \in \mathbb{Z}^+$, I_n is the identity matrix of size n, and $\mathbb{1}_n$ and 0_n the vectors of all ones and zeros in $\mathbb{R}^n$, respectively. Given a vector $v \in \mathbb{R}^n$, $\text{diag}(v) \in \mathbb{R}^{n\times n}$ is the diagonal matrix whose i-th diagonal element is the i-th entry of v. Given $v_1, \dots, v_p \in \mathbb{R}^n$, we denote $[v_1, \dots, v_p]$ and $[v_1; \dots; v_p]$ their horizontal and vertical concatenations. Given a matrix $A \in \mathbb{R}^{n\times m}$, A^T is its transpose, and $\|A\|_F$ its Frobenius norm. If A is square $(n = m)$, $\text{spec}(A)$ is its spectrum, $\lambda_i(A) \in \text{spec}(A)$ its i-th eigenvalues, $\lambda_{\min}(A)$ and $\lambda_{\max}(A)$ its eigenvalues with smallest and largest real part, respectively, and $\sigma_i(A)$ and $\underline{\sigma}(A)$ its i-th and smallest singular value, respectively. Given $A \in \mathbb{R}^{a\times b}$, $B \in \mathbb{R}^{c\times d}$, $(A \otimes B) \in \mathbb{R}^{ac\times bd}$ and $(A \oplus B) \in \mathbb{R}^{ac\times bd}$ are their Kronecker product and sum [22], respectively. Given a vector field $\varphi(z, w) : \mathbb{R}^a \times \mathbb{R}^b \to \mathbb{R}^n$, $D_z\varphi \in \mathbb{R}^{n\times a}$ and $D_w\varphi \in \mathbb{R}^{n\times b}$ are its Jacobian matrices with respect to z and w, respectively.

II. Directed Hypergraphs

A directed hypergraph $\mathscr{H}$ is a pair $(\mathcal{V}, \mathcal{E})$, with $\mathcal{V}$ the set of its nodes and $\mathcal{E}$ the set of its hyperedges. A hyperedge is a pair of ordered, disjoint subsets of $\mathcal{V}$. The first subset contains the *tails*, and the second its *heads* [18]. We call $\mathcal{T}(\epsilon)$ and $\mathcal{H}(\epsilon)$ the tail and head sets of the hyperedge ϵ, respectively, and indicate their cardinality with $|\mathcal{T}(\epsilon)|$ and $|\mathcal{H}(\epsilon)|$. Given two subsets $\mathcal{V}_1$ and $\mathcal{V}_2$ of $\mathcal{V}$, $\mathcal{E}^{\mathcal{V}_1,\mathcal{V}_2}$ is $\{\epsilon \in \mathcal{E} : \mathcal{V}_1 \subseteq \mathcal{T}(\epsilon) \wedge \mathcal{V}_2 \subseteq \mathcal{H}(\epsilon)\}$. If one of the two subsets is a singleton, we use the notation $\mathcal{E}^{j,\mathcal{V}_2}$, where j is the index related to the unique node of $\mathcal{V}$ in $\mathcal{V}_1$. Finally, $\mathcal{E}^{*,j} = \{\epsilon \in \mathcal{E} : v_j \in \mathcal{H}(\epsilon)\}$ is the subset of $\mathcal{E}$ having v_j as a head. Note that the main difference with standard graphs is that a hyperedge may have multiple tails and multiple edges, whereas in digraphs edges only have a single tail and a single head, as illustrated in Fig. 1.

III. Problem Formulation

Let us consider a controlled network of $N+1$ nonidentical dynamical systems coupled through a directed hypergraph $\mathscr{H} = \{\mathcal{V}, \mathcal{E}\}$, with node $N+1$ being the pinner that sets the reference trajectory for the network. The hyperedge set can be decomposed as $\mathcal{E} = \mathcal{E}_{\text{uc}} \cup \mathcal{E}_p$, where $\mathcal{E}_{\text{uc}}$ contains the hyperedges connecting the first N (controlled) nodes, and $\mathcal{E}_p$ contains the pinning hyperedges, whose sole tail is the pinner. Considering higher-order interactions and parameter mismatches, the classical equation (1) generalizes to

$$\dot{x}_i = f(x_i, \mu_i) + \sum_{\epsilon\in\mathcal{E}_{\text{uc}}^{*,i}} \sigma_\epsilon g\left(y_\epsilon^\tau \alpha_\epsilon - y_\epsilon^h \beta_\epsilon\right) + \sum_{\epsilon\in\mathcal{E}_p^{*,i}} k_\epsilon g\left(y_{N+1} - y_\epsilon^h \beta_\epsilon\right), \quad i = 1, \dots, N, \tag{2a}$$

$$y_i = \gamma(x_i), \qquad i = 1, \dots, N, \tag{2b}$$

$$\dot{x}_{N+1} = f(x_{N+1}, \bar{\mu}), \qquad y_{N+1} = \gamma(x_{N+1}) \tag{2c}$$

where vectors α_ϵ and β_ϵ stack the weights of the tails and heads of hyperedge ϵ, respectively, and are such that $\alpha_\epsilon^T \mathbb{1}_{|\mathcal{T}(\epsilon)|} = \beta_\epsilon^T \mathbb{1}_{|\mathcal{H}(\epsilon)|} = 1$; this implies $\alpha_\epsilon = 1$ for all $\epsilon \in \mathcal{E}_p$ as the pinner is the sole tail of the hyperedges it belongs to; $y_\epsilon^\tau \in \mathbb{R}^{m\times|\mathcal{T}(\epsilon)|}$ and $y_\epsilon^h \in \mathbb{R}^{m\times|\mathcal{H}(\epsilon)|}$ are matrices whose columns are vectors containing the outputs of the nodes that are tails and heads of hyperedge ϵ, respectively; for a hyperedge $\epsilon \in \mathcal{E}_{\text{uc}}$, σ_ϵ is its coupling strength, and for $\epsilon \in \mathcal{E}_p$, k_ϵ is the control gain of the associated feedback control action. Note that this model has several key differences with the classical model in (1). Indeed, as in [18], [19], [20]

1) The interactions take place within groups of nodes, and not only between pairs;
2) for any hyperedge $\epsilon \in \mathcal{E}$, a signal is transmitted from each tail to each head in ϵ; this signal will be a function of the difference between a convex combination of the outputs of the tails and a convex combination of the outputs of the heads.

Moreover, differently from the model in [18], [19], [20],

3) the individual dynamics differ from node to node for a vector of p parameters, which in (2) is denoted μ_i and will be the second argument of vector field $f : \mathbb{R}^n \times \mathbb{R}^p \to \mathbb{R}^n$ associated to node i;
4) the pinner node will not only define the reference trajectory, but will also be endowed with the nominal vector of parameters $\bar{\mu}$.

We define the trajectories error variables and parametric error variables with respect to the references set by the pinner:

$$e_i = x_i - x_{N+1}, \qquad \delta\mu_i = \mu_i - \bar{\mu}. \tag{3}$$

Introducing the stacks $e = [e_1; \dots; e_N]$ and $\delta\mu = [\delta\mu_1; \dots; \delta\mu_N]$, we can now provide the following definition:

Definition 1: The controlled network (2) is locally bounded pinning controlled if there is a $c \geq 0$ such that

a) for each $\varepsilon > c$, there are scalars $\Delta_1^x(\varepsilon)$, $\Delta_1^\mu(\varepsilon)$ such that

$$\|e(t)\| < \varepsilon, \quad \forall t \geq 0$$

for $\|e(0)\| < \Delta_1^x(\varepsilon)$, $\|\delta_\mu\| < \Delta_1^\mu(\varepsilon)$; and

b) there are scalar constants Δ_2^x, Δ_2^μ such that

$$\limsup_{t\to+\infty} \|e(t)\| \le c$$

for $\|e(0)\| < \Delta_2^x$, $\|\delta_\mu\| < \Delta_2^\mu$.

Problem statement. We seek for sufficient conditions guaranteeing that the network (2) is locally bounded pinning controlled. Moreover, we will also seek for an estimate $\tilde{c}$ of the bound c that is in principle valid only for local perturbations. Finally, we will test robustness of this estimate through numerical simulations for increasing values of the parameter mismatch vector $\delta\mu$.

IV. Main Results

A. Linearization and Block Diagonalization

Lemma 1 [18]: Given any hyperedge $\epsilon \in \mathcal{E}$, we have

$$y_\epsilon^\tau \alpha_\epsilon - y_\epsilon^h \beta_\epsilon = \sum_{j\in\mathcal{T}(\epsilon)} (\tilde{\alpha}_\epsilon)_j (y_j - y_i) - \sum_{j\in\mathcal{H}(\epsilon)} \left(\tilde{\beta}_\epsilon\right)_j (y_j - y_i) \tag{4}$$

where the jth entry of $\tilde{\alpha}_\epsilon$ $(\tilde{\beta}_\epsilon)$ is 0 if node j is not a tail (head), whereas it is equal to the weight associated to the corresponding tail (head), otherwise.

By leveraging Lemma 1, we substitute (4) into (2a), and, from the definition of e_i in (3), obtain

$$\begin{aligned}\dot{e}_i =& f(x_i,\mu_i) - f(x_{N+1},\bar{\mu}) + \sum_{\epsilon\in\mathcal{E}_{\mathrm{uc}}^{*,i}} \sigma_\epsilon g\Bigg(\sum_{j\in\mathcal{T}(\epsilon)} (\tilde{\alpha}_\epsilon)_j \big(\gamma(x_j) \\ &- \gamma(x_i)\big) - \sum_{j\in\mathcal{H}(\epsilon)} \left(\tilde{\beta}_\epsilon\right)_j \big(\gamma(x_j) - \gamma(x_i)\big)\Bigg) \\ &+ \sum_{\epsilon\in\mathcal{E}_p^{*,i}} k_\epsilon g\Bigg(\gamma(x_{N+1}) - \gamma(x_i) - \sum_{j\in\mathcal{H}(\epsilon)} \left(\tilde{\beta}_\epsilon\right)_j \big(\gamma(x_j) - \gamma(x_i)\big)\Bigg).\end{aligned} \tag{5}$$

Using that $x_i = x_{N+1} + e_i$ and $\mu_i = \bar{\mu} + \delta\mu_i$, we linearize eq. (5) around the synchronization manifold $x_1 = \ldots = x_N = x_{N+1}$ and the nominal parameter values $\bar{\mu}$. Considering the first-order expansion of f around $(x_{N+1}, \bar{\mu})$, of γ around x_{N+1}, and of g around 0, and using the symbol $\tilde{e}$ to denote the linearized error dynamics, one obtains

$$\begin{aligned}\dot{\tilde{e}}_i =& D_x f(x_{N+1},\bar{\mu})\tilde{e}_i + \sum_{\epsilon\in\mathcal{E}_{\mathrm{uc}}^{*,i}} \sigma_\epsilon H(x_{N+1}) \\ &\left(\sum_{j\in\mathcal{T}(\epsilon)} (\tilde{\alpha}_\epsilon)_j (\tilde{e}_j - \tilde{e}_i) - \sum_{j\in\mathcal{H}(\epsilon)} \left(\tilde{\beta}_\epsilon\right)_j (\tilde{e}_j - \tilde{e}_i)\right) \\ &+ \sum_{\epsilon\in\mathcal{E}_p^{*,i}} k_\epsilon H(x_{N+1}) \left(-\tilde{e}_i - \sum_{j\in\mathcal{H}(\epsilon)} \left(\tilde{\beta}_\epsilon\right)_j (\tilde{e}_j - \tilde{e}_i)\right) \\ &+ D_\mu f(x_{N+1},\bar{\mu})\delta\mu_i,\end{aligned} \tag{6}$$

where $H(x_{N+1}) = D_x g(0) D_x \gamma(x_{N+1})$, and we considered that $g(0) = 0$. Next, we rewrite (6) as

$$\begin{aligned}\dot{\tilde{e}}_i =& D_x f(x_{N+1},\bar{\mu})\tilde{e}_i + H(x_{N+1}) \\ &\left(\sum_{j=1}^N s_{ij}(\tilde{e}_j - \tilde{e}_i) - \sum_{\epsilon\in\mathcal{E}_p^{N+1,i}} k_\epsilon \tilde{e}_i\right) \\ &+ D_\mu f(x_{N+1},\bar{\mu})\delta\mu_i\end{aligned} \tag{7}$$

where

$$s_{ij} = \sum_{\epsilon\in\mathcal{E}_{\mathrm{uc}}^{j,i}} (\tilde{\alpha}_\epsilon)_j \sigma_\epsilon - \sum_{\epsilon\in\mathcal{E}_{\mathrm{uc}}^{*,\{i,j\}}} \left(\tilde{\beta}_\epsilon\right)_j \sigma_\epsilon - \sum_{\epsilon\in\mathcal{E}_p^{N+1,\{i,j\}}} \left(\tilde{\beta}_\epsilon\right)_j k_\epsilon \tag{8}$$

for all $i, j = 1, \ldots, N$. The scalar s_{ij} can be viewed as the entry ij of the adjacency matrix S associated to a signed graphs, as from (8) s_{ij} can also be negative. The Laplacian matrix associated to S will be $L = \mathrm{diag}(S\mathbb{1}_N) - S$, and is then zero row-sum, thereby having a zero eigenvalue with associated eigenvector $\mathbb{1}_N$, but, unlike Laplacians of positively weighted digraphs, may also have negative real-part eigenvalues [23]. We then introduce matrix M whose ij-th entry m_{ij} is equal to $l_{ij} + \sum_{\epsilon\in\mathcal{E}_p^{N+1,i}} k_\epsilon$ if $i = j$, and it is equal to l_{ij} otherwise. As we assume that the set of pinning hyperedges $\mathcal{E}_p$ is not empty, M will not be zero row-sum, and therefore, differently from L, will not be endowed with the eigenpair $(0, \mathbb{1}_N)$. We can then rewrite eq. (7) as

$$\begin{aligned}\dot{\tilde{e}}_i =& D_x f(x_{N+1},\bar{\mu})\tilde{e}_i - H(x_{N+1}) \sum_{j=1}^N m_{ij}\tilde{e}_j \\ &+ D_\mu f(x_{N+1},\bar{\mu})\delta\mu_i\end{aligned} \tag{9}$$

and describe the dynamics of $\tilde{e} = [\tilde{e}_1; \ldots; \tilde{e}_N]$ as

$$\dot{\tilde{e}} = \left[I_N \otimes D_x f - M \otimes H\right]\tilde{e} + \left(I_N \otimes D_\mu f\right)\delta\mu. \tag{10}$$

Next, consider the real Jordan transformation matrix T_r such that $M = T_r J_r T_r^{-1}$, where J_r is a block diagonal matrix, with each diagonal block associated to a real eigenvalue of M, or to a pair of complex eigenvalues of M. For a generic pair of complex conjugate eigenvalues $\alpha_i \pm \imath\omega_i$ in spec(M), the corresponding diagonal block $(J_r)_i \in \mathbb{R}^{2b_i\times 2b_i}$ of J_r, with b_i being the size of the Jordan block associated to λ_i, is

$$(J_r)_i = \begin{bmatrix} S_i & 0_{2\times2} & & & \\ I_2 & S_i & 0_{2\times2} & & \\ & \ddots & \ddots & \ddots & \\ & & I_2 & S_i & 0_{2\times2} \\ & & & I_2 & S_i \end{bmatrix}, \tag{11}$$

where the diagonal sub-block $S_i = [\alpha_i, \omega_i; -\omega_i, \alpha_i]$ is repeated b_i times. If, instead, λ_i is real, then $(J_r) \in \mathbb{R}^{b_i\times b_i}$ and coincides with the Jordan block associated to λ_i, that is,

$$(J_r)_i = \begin{bmatrix} \lambda_i & 0 & & \\ 1 & \ddots & \ddots & \\ & \ddots & \ddots & 0 \\ & & 1 & \lambda_i \end{bmatrix} \tag{12}$$

We denote with ζ the number of diagonal blocks of J_r, and, without loss of generality, choose T_r so that the first r blocks will be associated with real eigenvalues, whereas the last $\zeta - r$ will be associated to a pair of complex conjugate eigenvalues.

We now define the following time-varying matrices:

$$A_i(t) = \begin{cases} D_x f - \lambda_i(M)H, i = 1, \ldots, r, \\ \begin{bmatrix} D_x f - \alpha_i H & -\omega_i H \\ \omega_i H & D_x f - \alpha_i H \end{bmatrix}, \\ i = r+1, \ldots, \zeta, \end{cases} \tag{13}$$

where we note that the dependency on time of A_i stands in the dependence of both $D_x f$ and H on $x_{N+1}(t)$, which we omitted for brevity. By assuming that the eigenvalues of $A_i(t)$ have negative real-part for all $t \geq 0$, we can define the positive symmetric time-varying matrix $P_i(t)$ that is the solution of the Lyapunov equation

$$A_i(t)^T P_i(t) + P_i(t) A_i(t) = -Q_i, \qquad \forall t \geq 0 \tag{14}$$

where Q_i is a constant and positive definite matrix. Next,

$$\widetilde{H}_i = \begin{cases} H, & i = 1, \dots, r, \\ I_2 \otimes H, & i = r+1, \dots, \zeta, \end{cases} \tag{15}$$

the time-varying matrix

$$B_i(t) = \begin{cases} D_\mu f(x_{N+1}(t), \bar{\mu}), & i = 1, \dots, r, \\ I_2 \otimes D_\mu f(x_{N+1}(t), \bar{\mu}), & i = r+1, \dots, \zeta, \end{cases} \tag{16}$$

and, for all $j = 1, \dots, b_i$,

$$u_{ij} = \begin{cases} \sum_{k=1}^{N} \tau_{(l_i+j-1)k} \delta\mu_k, & i = 1, \dots, r, \\ \left[\sum_{k=1}^{N} \tau_{(l_i+2j-2)k} \delta\mu_k; \sum_{k=1}^{N} \tau_{(l_i+2j-1)k} \delta\mu_k \right], & \\ \qquad i = r+1, \dots, \zeta, \end{cases} \tag{17}$$

where τ_{ij} is the ij-th entry of T_r^{-1}, $l_i = 1 + \sum_{j=1}^{i-1} \gamma_j$, with γ_j being the size of the j-th block of J_r ($\gamma_j = b_j$ if the j-th block is associated to a real eigenvalue, whereas $\gamma_j = 2b_j$, otherwise). By applying the change of variables $\eta = (T_r^{-1} \otimes I_n)\tilde{e}$, from eq. (10) we obtain

$$\dot{\eta} = \left[I_N \otimes D_x f - J_r \otimes H \right] \eta + \left(T_r^{-1} \otimes D_\mu f \right) \delta\mu \tag{18}$$

Proving boundedness of η is equivalent to prove that network (2) is locally bounded pinning controlled. We can write $\eta = [\eta_1; \dots; \eta_r; \eta_{r+1}, \dots, \eta_\zeta]$, where $\eta_i = [\eta_{i1}; \dots; \eta_{ib_i}]$ is associated to the i-th block of J_r, with $\eta_{ij} \in \mathbb{R}^n$ if the i-th block is associated to a real eigenvalue ($i \leq r$), and $\eta_{ij} \in \mathbb{R}^{2n}$ otherwise ($i > r$). For all $i = 1, \dots, \zeta$, the dynamics of η_i can be written as

$$\begin{aligned} \dot{\eta}_{i1} &= A_i(t)\eta_{i1} + B_i(t) u_{i1}, \\ \dot{\eta}_{i2} &= A_i(t)\eta_{i2} - \widetilde{H}_i \eta_{i1} + B_i(t) u_{i2}, \\ &\vdots \\ \dot{\eta}_{ib_i} &= A_i(t)\eta_{ib_i} - \widetilde{H}_i \eta_{i(b_i-1)} + B_i(t) u_{ib_i}. \end{aligned} \tag{19}$$

Finally, assuming that $P_i(t)$ in (14), $\widetilde{H}_i$ in (15), and $B_i(t)$ in (16) are uniformly bounded in norm, and given scalars $\varsigma_1, \dots, \varsigma_\zeta$ in the open interval $]0, 1[$, we can define the following scalars, which, for all $i = 1, \dots, \zeta$, can be simultaneously computed as

$$\begin{aligned} a_{i1} &= 2P^i_{\max} B^{i1}_{\max}, \\ \kappa_i &= (1 - \varsigma_i)\underline{\sigma}(Q_i), \; c_{ij} = a_{ij}/\kappa_i, & j = 1, \dots, b_i, \\ a_{ij} &= 2P^i_{\max} B^{ij}_{\max} + c_{i,(j-1)} \widetilde{H}^i_{\max}, & j = 2, \dots, b_i \end{aligned} \tag{20}$$

where Q_i is the positive definite matrix in (14), and

$$P^i_{\max} = \limsup_{t \to +\infty} \|P_i(t)\|, \; B^{ij}_{\max} = \limsup_{t \to +\infty} \|B_i(t) u_{ij}\|,$$
$$\widetilde{H}^i_{\max} = \limsup_{t \to +\infty} \|\widetilde{H}_i(t)\|.$$

B. Local Bounded Pinning Controllability

Theorem 1: If, for all $i = 1, \dots, \zeta$,

(H1) $\Re(\lambda_k(A_i(t))) < 0$, for all $t \geq 0$, $i = 1, \dots, q$, and $k = 1, \dots, |\mathrm{spec}(A_i(t))|$,

(H2) $A_i(t)$ is differentiable and uniformly bounded in norm,

(H3) there exist a positive definite matrix Q_i with the same size as $A_i(t)$, and a positive scalar $\varsigma_i < 1$ such that

$$\|\dot{A}_i(t)\| \leq \frac{\varsigma_i \underline{\sigma}^2(A_i(t) \oplus A_i(t)) \underline{\sigma}(Q_i)}{2\|Q_i\|_F} \tag{21}$$

(H4) $B_i(t)$ is uniformly bounded in norm,

then the controlled network (2) over a directed hypergraph $\mathscr{H}$ is locally bounded pinning controlled. Additionally,

$$\limsup_{t \to +\infty} \|\tilde{e}\| \leq \tilde{c} = \|T_r\| \left\| \left[c_1, \dots, c_\zeta \right] \right\| \tag{22}$$

with $c_i = \|[c_{i1}, \dots, c_{ib_i}]\|$, for all $i = 1, \dots, \zeta$.

Proof: We show bounded convergence of each η_i, $i = 1, \dots, \zeta$. As the dynamic matrix for η_i is block-triangular, we can study its bounded convergence algorithmically, by first deriving a bound on η_{i1}, to then derive the bound for η_{ij} as a function of the bound for $\eta_{i(j-1)}$, for all $j = 2, \dots, b_i$. Hence, we start with η_{i1} and consider the following Lyapunov function candidate with time-varying kernel:

$$V(\eta_{i1}) = \eta_{i1}^T P_i(t) \eta_{i1} \tag{23}$$

where $P_i(t)$ is the solution of (14), which exists from H1. By omitting the explicit dependence on time, we have

$$\begin{aligned} \dot{V}(\eta_{i1}) &= \left[\left(\eta_{i1}^T A_i^T + u_{i1}^T B_i^T \right) P_i + \eta_{i1}^T \dot{P}_i \right] \eta_{i1} \\ &\quad + \eta_{i1}^T P_i (A_i \eta_{i1} + B_i u_{i1}) \end{aligned} \tag{24}$$

From (14), and bounding $\dot{P}_i$ with $||\dot{P}_i|| I_n$, we obtain

$$\begin{aligned} \dot{V}(\eta_{i1}) &= -\eta_{i1}^T \left(Q_i - \dot{P}_i \right) \eta_{i1} + 2\eta_{i1}^T P_i B_i u_{i1} \\ &\leq -\left(\underline{\sigma}(Q_i) - \|\dot{P}_i\| \right) \|\eta_{i1}\|^2 + 2\eta_{i1}^T P_i B_i u_{i1}. \end{aligned} \tag{25}$$

From [24] we know that

$$\|\dot{P}_i(t)\| \leq \frac{2\|\dot{A}_i(t)\| \|Q_i\|_F}{\underline{\sigma}^2(A_i(t) \oplus A_i(t))} \tag{26}$$

From H2, $A_i(t)$ is uniformly bounded, and then the right-end side of (26) will also be bounded, thereby implying that there exists a scalar $P^i_{\max} = \limsup_{t \to \infty} \|\dot{P}_i(t)\|$. Moreover, by combining (25) and (26), using the properties of vector and matrix 2-norms, and from hypothesis H3-H4, we obtain

$$\dot{V}(\eta_{i1}) \leq -(1 - \varsigma_i)\underline{\sigma}(Q_i) \|\eta_{i1}\|^2 + 2P^i_{\max} B^{i1}_{\max} \|\eta_{i1}\|. \tag{27}$$

We note that $\dot{V}(\eta_{i1}) < 0$ for all η_{i1} such that $\|\eta_{i1}\| > a_{i1}/\kappa_i$, thereby implying that

$$\limsup_{t \to +\infty} \|\eta_{i1}\| \leq a_{i1}/\kappa_i = c_{i1} \tag{28}$$

where a_{i1}, κ_i, and c_{i1} are defined in (20).

The bound (28) is used to trigger an algorithmic procedure that computes all the bounds for $\eta_{i2}, \dots, \eta_{ib_i}$. Namely, we assume to have already computed a bound for $\|\eta_{i(j-1)}\|$, so $\limsup_{t \to +\infty} \|\eta_{i(j-1)}\| \leq c_{i(j-1)}$, and then use it to compute the bound for $\|\eta_{ij}\|$. Then, we proceed with the same Lyapunov function candidate $V(\eta_{ij}) = \eta_{ij}^T P_i(t) \eta_{ij}$ as in (23). By deriving

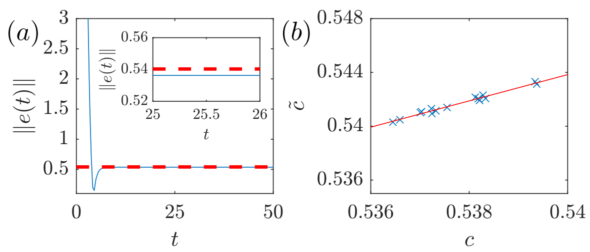

Fig. 2. (a) Dynamics of the error norm when community C_4 is pinned, and (b) linear fit of the estimated bound $\tilde{c}$ versus the actual one from simulations c, computed when each of the 15 communities are pinned. Correlation between $\tilde{c}$ and c is 0.99, with p-value smaller than 10^{-3}.

it with respect to time, the same line of argument as for $\dot{V}(\eta_{i1})$, and the bound on $\eta_{i,(j-1)}$, yield

$$\dot{V}(\eta_{ij}) \leq -\kappa_i \|\eta_{ij}\|^2 + a_{ij}\|\eta_{ij}\|, \qquad j = 2, \dots, b_i \tag{29}$$

where a_{ij} and κ_i are defined in (20).

By combining (27) and (29), one finally obtains that

$$\limsup_{t\to+\infty} \|\eta_i\| \leq c_i \tag{30}$$

where $c_i = \|[c_{i1}; \dots; c_{ib_i}]\|$. Since (30) holds for all $i = 1, \dots, \zeta$, we then obtain

$$\limsup_{t\to+\infty} \|\eta\| \leq \big\|[c_1, \dots, c_\zeta]\big\|. \tag{31}$$

Since $\tilde{e} = (T_r \otimes I_n)\eta$, we then obtain (22). This implies local boundedness of (5) and, in turn, that (2) is locally bounded pinning controlled. ■

Remark 1: The assumption of Theorem 1 are mild: from (13) and (16), H2 and H4 are always fulfilled if f, γ and h are sufficiently smooth, as both A_i and B_i are evaluated at a bounded solution $x_{N+1}(t)$ of the nominal dynamics, i.e., the reference trajectory set by the pinner. Sufficient smoothness of f and γ also guarantees boundedness of $\|\dot{A}_i(t)\|$, thereby favoring the fulfilment of H3. Finally, H1 requires finding the right coupling and control gains to make $A_1, \dots, A_\zeta$ Hurwitz, and in the next corollary we will see a condition when the gains can be easily designed.

When the output and inner coupling functions are the identity, and all coupling and control gains are equal ($\sigma_\varepsilon = \sigma$ for all $\varepsilon \in \mathcal{E}_{uc}$, and $k_\varepsilon = k$ for all $\varepsilon \in \mathcal{E}_p$), we define a backbone signed adjacency matrix $\widetilde{S}$ (with associated backbone Laplacian $\widetilde{L}$) whose entry ij can be obtained by dividing the right-end side of (8) by σ. A (non-zero row-sum) backbone matrix $\widetilde{M}$ is obtained by adding $\sum_{\varepsilon\in\mathcal{E}_p^{N+1,i}} \chi$ to its diagonal entry ii, for $i = 1, \dots, N$, with $\chi = k/\sigma$.

Corollary 1: If H2, H3, and H4 hold, and

(H1b) $\sigma_\varepsilon = \sigma$ for all $\varepsilon \in \mathcal{E}_{\text{uc}}$, $k_\varepsilon = k$ for all $\varepsilon \in \mathcal{E}_p$, $\Re(\lambda_{\min}(\widetilde{M})) > 0$, γ and g are the identity function,

$$\sigma > \frac{\limsup_{t\to+\infty} \Re\big(\lambda_{\max}(D_x f(x_{N+1}(t), \bar{\mu}))\big)}{\Re\big(\lambda_{\min}(\widetilde{M})\big)} \tag{32}$$

the controlled network (2) over a directed hypergraph $\mathscr{H}$ is locally bounded pinning controlled and bound (22) holds.

Proof: We use the change of variable $\eta = (T^{-1} \otimes I_n)\tilde{e}$, with T such $M = TJT^{-1}$, $\eta = [\eta_1, \dots, \eta_b]$, J the Jordan matrix associated to M, and b the number of its blocks. The dynamic matrix of the first n variables of each η_i will be $D_x f(x_{N+1}(t), \bar{\mu}) - \sigma\lambda_i(\widetilde{M})I_n$. From norm equivalences, and from H2, $\limsup_{t\to+\infty} \Re(\lambda_{\max}(D_x f(x_{N+1}(t), \bar{\mu})))$ is finite, thus the right-end side of (32) is also finite. Hence, for all σ satisfying (32), H1 of Theorem 1 is fulfilled. ■

V. Numerical Examples

1) Opinion Dynamics: we consider a network of $N = 150$ people that need to form an opinion on a two-option choice (e.g., a referendum) influenced by an opinion leader, the pinner [25]. Each person has its own opinion x_i, with $x_i = 0$ corresponding to a neutral opinion, and $x_i > 0$ and $x_i < 0$ to an agent leaning toward option 1 or option 2, respectively. The larger $|x_i|$ the more extreme will be the opinion of agent i. The individual dynamics of each agent are $f(x_i, \mu_i) = -3x_i + \mu_i \tanh(x_i)$, where the parameter $\mu_i > 3$ describes the *extremism* of agent i. Indeed, for $\mu_i > 3$, individual dynamics have an unstable equilibrium in 0 and two stable equilibria in $\pm\bar{x}_i$, with $\bar{x}_i$ being more extreme the larger μ_i is. The initial opinions of each agent are uniformly drawn in $[-\bar{x}_{\max}, \bar{x}_{\max}]$, where $\bar{x}_{\max} = \max_i \bar{x}_i$.

Coupling term: we extracted the topology from the hypergraph of social interactions in [26], where each hyperedge represents a group interaction between individuals, and we set $\sigma_\epsilon = 1$ for all $\epsilon \in \mathcal{E}_{\text{uc}}$. Moreover, each edge or tail has the same importance, $(\alpha_\epsilon)_i = 1/|\mathcal{T}(\epsilon)|$ and $(\beta_\epsilon)_i = 1/|\mathcal{H}(\epsilon)|$ in (2) for all i, and $\gamma(x_i) = x_i$ and $g(x_i) = x_i$. The 150 followers are grouped in 15 communities $C_1, \dots, C_{15}$ of 10 nodes each, with few cross-community links.

Parameter mismatches: μ_i is drawn from a uniform distribution in [3.2, 4.8], and represents different extremism levels.

Pinning control: the pinner is the opinion leader, with $\mu_{N+1} = 4$, that tries to steer the opinions of the followers towards its reference opinion. Having limited resources, it is constrained to pin (influence) only one community. We choose to pin community C_4 as, according to Theorem 1, this yields the smallest bound estimate $\tilde{c}$, which is a good approximation of the numerical one, see Fig. 2(a). The accuracy of the estimation is testified by the strong correlation coefficient between $\tilde{c}$ and c, see Fig. 2(b).

2) Network of $N = 100$ Rössler Systems: the individual dynamics are $f(x_i, \mu_i) = [-x_{i2} - x_{i3}; x_{i1} + \mu_{i1}x_{i2}; \mu_{i2} + x_{i3}(x_{i1} - \mu_{i3})]$, with the nominal parameter values being $\bar{\mu} = [0.2; 0.2; 5.6]$, and initial conditions taken randomly in the chaotic attractor. Furthermore, the output and inner coupling function are $\gamma(x_i) = x_i$ and $g(x_i) = x_i$.

Coupling hypergraph. We couple the nodes through an Erdös-Rényi like hypergraph with only pairwise and triadic interactions, and with the parameter p modulating the number of hyperedges set to 0.1 [20]. All hyperedges in $\mathcal{E}_{\text{uc}}$ are undirected with identical weights $\sigma_\epsilon = 50$ for all $\epsilon \in \mathcal{E}_{\text{uc}}$, and we set $(\alpha_\epsilon)_i = 1/|\mathcal{T}(\epsilon)|$ and $(\beta_\epsilon)_i = 1/|\mathcal{H}(\epsilon)|$ in (2) for all i. The pinner sets the reference trajectory but cannot measure the state of each node: each pinning hyperedge has 2 head nodes of which the pinner measures the average state, i.e., $\beta_\epsilon = [0.5; 0.5]$, $\forall\epsilon \in \mathcal{E}_p$, and 1 tail, the pinner itself.

Control gain selection and robustness of estimated bound. We consider two cases, in which 20 or 50 control hyperedges are added, respectively. To fulfil the hypotheses of Corollary 1, k should be larger than 11.8 and 4.7, respectively, so that the right-end side of (32) becomes smaller than $\sigma = 50$. Thus, we set $k_\epsilon = 50$ for all $\epsilon \in \mathcal{E}_p$ for both cases. Further, we assume that the parameter μ_{ij} is drawn from a uniform distribution in $[\bar{\mu}_j(1 - \psi), \bar{\mu}_j(1 + \psi)]$, for $i = 1, \dots, N$, and $j = 1, 2, 3$, so increasing ψ increases the relative amplitude of the parameter mismatches. Fig. 3 reports the dynamics of the error norms for $\psi = 0.5$ (the parameters can vary up to 50% of their nominal value), and we note how the bound estimated in (22) holds and

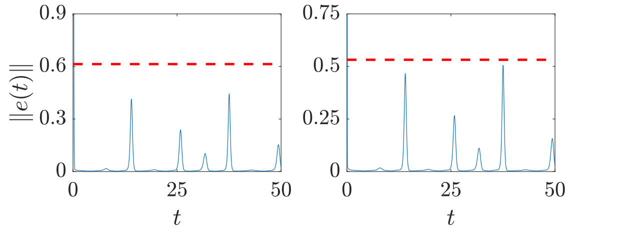

Fig. 3. Controlled network of $N = 100$ nodes coupled through an Erdös-Rényi like random hypergraph. Sample dynamics of the error norm when 20 (left panel) or 50 (right panel) pinning hyperedges of size 3 are considered. The red dashed lines depict the theoretical bounds computed from (22).

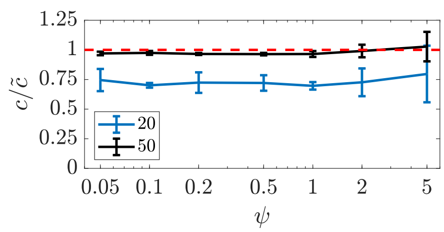

Fig. 4. Controlled network of $N = 100$ nodes coupled through an Erdös-Rényi like random hypergraph. Ratio between the numerically obtained bound c and the bound $\tilde{c}$ from (22) when 20 (in blue) or 50 (in black) control hyperedges are used. The red dashed line corresponds to perfect matching between c and $\tilde{c}$, and error bars to one standard deviation.

is tight. We then test the validity of the estimated bound, based on linearization, for increasing parameter mismatches and vary ψ between 0.05 and 5. For each ψ, we run 10 simulations differing for the randomly generated coupling hypergraph and record both $\tilde{c}$ and the actual bound c observed in simulation. We note that the estimated bound holds ($c \leq \tilde{c}$) in 98.8% of the cases, and may be violated only when parameters can vary up to 100% with respect to the nominal values, see Fig. 4, when the individual node dynamics can also diverge if uncoupled.

VI. Conclusion

We have provided for the first time rigorous conditions guaranteeing local bounded pinning controllability in networks of nonidentical systems coupled through a directed hypergraph. Indeed, previous global results would not hold in the presence of parameter mismatches [18], [19]. Instead of pursuing an approach based on the master stability function [20], which could only yield semi-analytical results requiring the simulation of the network dynamics, our methodology allowed to provide a) closed-form conditions for local bounded pinning control that can be checked off-line, and b) a bound on the linearized dynamics which is useful beyond the case of infinitesimal perturbations. Indeed, we numerically showed a) the robustness of the bound, still fulfilled even for perturbations so large that would make the individual dynamics unstable, and b) how the bound estimated from linearization is strongly correlated with the actual one, and can be used as a proxy of the effectiveness of the control strategy.

Acknowledgment

This manuscript reflects only the authors' views and opinions and the Ministry cannot be considered responsible for them.

Open Access funding provided by 'Università degli Studi di Napoli "Federico II"' within the CRUI CARE Agreement

References

[1] R. M. D'Souza, M. di Bernardo, and Y.-Y. Liu, "Controlling complex networks with complex nodes," *Nat. Rev. Phys.*, vol. 5, no. 4, pp. 250–262, 2023.

[2] F. Della Rossa and P. De Lellis, "Synchronization and pinning control of stochastic coevolving networks," *Annu. Rev. Control*, vol. 53, pp. 147–160, 2022. [Online]. Available: https://www.sciencedirect.com/science/article/pii/S1367578822000207

[3] W. Yu, G. Chen, and J. Lü, "On pinning synchronization of complex dynamical networks," *Automatica*, vol. 45, no. 2, pp. 429–435, 2009.

[4] J. Zhou, J.-A. Lu, and J. Lü, "Pinning adaptive synchronization of a general complex dynamical network," *Automatica*, vol. 44, no. 4, pp. 996–1003, 2008.

[5] V. Gazi and K. M. Passino, "Stability analysis of swarms," *IEEE Trans. Autom. Control*, vol. 48, no. 4, pp. 692–697, Apr. 2003.

[6] R. Carli et al., "Consensus-based algorithms for controlling swarms of unmanned aerial vehicles," in *Proc. 19th ADHOC-NOW*, 2020, pp. 84–99.

[7] W. S. Rossi and P. Frasca, "Asynchronous opinion dynamics on the k-nearest-neighbors graph," in *Proc. IEEE CDC*, 2018, pp. 3648–3653.

[8] P. De Lellis, M. Ruiz Marín, and M. Porfiri, "Modeling human migration under environmental change: A case study of the effect of sea level rise in Bangladesh," *Earth's Future*, vol. 9, no. 4, 2021, Art. no. e2020EF001931.

[9] X. F. Wang and G. Chen, "Pinning control of scale-free dynamical networks," *Physica A Stat. Mech. Appl.*, vol. 310, nos. 3–4, pp. 521–531, 2002.

[10] W. Lu, X. Li, and Z. Rong, "Global stabilization of complex networks with digraph topologies via a local pinning algorithm," *Automatica*, vol. 46, no. 1, pp. 116–121, 2010.

[11] D. J. Hill and J. Zhao, "Global synchronization of complex dynamical networks with non-identical nodes," in *Proc. 47th CDC*, 2008, pp. 817–22.

[12] J. Montenbruck, M. Bürger, and F. Allgöwer, "Practical synchronization with diffusive couplings," *Automatica*, vol. 53, pp. 235–43, Mar. 2015.

[13] P. DeLellis, M. Di Bernardo, and D. Liuzza, "Convergence and synchronization in heterogeneous networks of smooth and piecewise smooth systems," *Automatica*, vol. 56, pp. 1–11, Jun. 2015.

[14] G. Bianconi, *Higher-Order Networks*. Cambridge, U.K.: Cambridge Univ. Press, 2021.

[15] S. Boccaletti et al., "The structure and dynamics of networks with higher order interactions," *Phys. Rep.*, vol. 1018, pp. 1–64, May 2023.

[16] D. Salzano, D. Fiore, and M. di Bernardo, "Ratiometric control of cell phenotypes in monostrain microbial consortia," *J. Roy. Soc. Interface*, vol. 19, no. 192, 2022, Art. no. 20220335.

[17] Q. Ouyang et al., "A unified model for active battery equalization systems," 2024, *arXiv:2403.03910*.

[18] P. De Lellis et al., "Pinning control of hypergraphs," *IEEE Control Syst. Lett.*, vol. 7, pp. 691–696, 2023, doi: 10.1109/LCSYS.2022.3217093.

[19] P. De Lellis, F. Della Rossa, F. L. Iudice, and D. Liuzza, "Pinning control of linear systems on hypergraphs," *Eur. J. Control*, vol. 74, Nov. 2023, Art. no. 100836.

[20] F. Della Rossa, D. Liuzza, F. Lo Iudice, and P. De Lellis, "Emergence and control of synchronization in networks with directed many-body interactions," *Phys. Rev. Lett.*, vol. 131, no. 20, 2023, Art. no. 207401.

[21] K. Kovalenko et al., "Contrarians synchronize beyond the limit of pairwise interactions," *Phys. Rev. Lett.*, vol. 127, Dec. 2021, Art. no. 258301.

[22] A. Graham, *Kronecker Products and Matrix Calculus With Applications*. Mineola, NY, USA: Dover Publ., 2018.

[23] S. Ahmadizadeh et al., "On eigenvalues of Laplacian matrix for a class of directed signed graphs," *Linear Algebra its Appl.*, vol. 523, pp. 281–306, Jun. 2017.

[24] F. Amato, G. Celentano, and F. Garofalo, "New sufficient conditions for the stability of slowly varying linear systems," *IEEE Trans. Autom. Control*, vol. 38, no. 9, pp. 1409–1411, Sep. 1993.

[25] F. Lo Iudice, F. Garofalo, and P. De Lellis, "Bounded partial pinning control of network dynamical systems," *IEEE Trans. Control Netw. Syst.*, vol. 10, no. 1, pp. 238–248, Mar. 2023.

[26] J. Stehlé et al., "High-resolution measurements of face-to-face contact patterns in a primary school," *PloS One*, vol. 6, no. 8, 2011, Art. no. e23176.